

Nature-Inspired Bacterial Cellulose/Methylglyoxal (BC/MGO) Nanocomposite for Broad-Spectrum Antimicrobial Wound Dressing

Manni Yang, John Ward, and Kwang-Leong Choy*

Bacterial cellulose (BC) is a natural material produced by *Acetobacter xylinum*, widely used in wound dressings due to the high water-holding capacity and great mechanical strength. In this paper, a novel antimicrobial dressing made from BC/methylglyoxal (MGO) composite with a dip-coating method inspired by naturally antimicrobial Manuka honey is proposed, which to our best knowledge, has not yet to be reported. Characterizations by scanning electron microscope and atomic force microscopy show the interconnected nanostructure of BC and MGO and increase surface roughness of the BC/MGO composite. Thermal analysis indicates high temperature stability of both BC and BC/MGO, while compared with BC, BC/MGO exhibits slightly weaker thermal stability possibly due to reduction of hydrogen bonding and increase of crystallinity. Mechanical test confirms the strong mechanical property of BC and BC/MGO nanocomposite. From the disk diffusion antimicrobial test, the BC/MGO nanocomposite with highest MGO concentration (4%) shows great zone inhibition diameter (around 14.3, 12.3, 17.1, and 15.5 mm against *Micrococcus luteus*, *Pseudomonas aeruginosa*, *Staphylococcus aureus*, and *Escherichia coli*). Compared with other antimicrobial wound dressing composite materials, the proposed BC/MGO nanocomposite has among the greatest antimicrobial property against broad-spectrum bacteria, making it a promising antimicrobial dressing in chronic wounds care.

1. Introduction

Bacterial cellulose (BC), also called microbial celluloses or bacterial nanocellulose, is a polysaccharide, produced by aerobic bacteria in both synthetic and nonsynthetic medium through oxidative fermentation.^[1] When compared to plant cellulose, BC has a unique structure solely consisting of glucose monomer, great properties are exhibited such as the unique nanostructure,^[2] high water-holding capacity,^[3] high degree of polymerization,^[4] high mechanical strength,^[5] high crystallinity,^[6] as well as biocompatibility and moisture ability for its ultrafine network structure of nonaggregated nanofibrils.^[7–9] Previous studies have revealed that BC as well as its derivatives are promising materials for application in various fields of biomedical, electronic, and food industries.^[10]


Wound dressings can accelerate the healing process and reduce the debris influence by providing the functions of both permeability and protection of regenerated tissues^[11,12] as well as maintaining suitable

hydration.^[13] Recent antimicrobial wound dressings are mainly made by sponges, hydrogels, hydrocolloids, and electrospinning membranes; however, those can have some drawbacks as sponges and hydrogel are often in poor mechanical strength which are not appropriate to treat wounds in late-stage,^[14–16] while hydrocolloids can exhibit toxicity as well as electrospinning membranes due to the solvents used in fabrication process.^[17–19] Therefore, a natural product such as BC is an excellent candidate for a dressing substrate. However, since BC has no antibacterial properties, the most important task is to introduce an antimicrobial property of BC. For wound infections, prevention of secondary infection and maintaining a suitable local environment has been proven to be the major issue in assisting the healing process.^[14] Various types of solutions have been employed to deal with the problem, including BC/chitosan,^[20] BC/silver nanoparticles (AgNP),^[21,22] BC/copper nanoparticles,^[23] BC/povidone-iodine, BC/polyhexamethylene biguanide (PHMB),^[24] and BC/tetracycline hydrochloride (TCH).^[25] However, some of the organic antimicrobial BC nanocomposites were just against Gram-positive bacteria, and those incorporated with Ag/AgNP are a threat because they can cause a danger to human health, such as Argyria or argyrosis.^[26]

M. Yang
Institute for Materials Discovery
Department of Chemistry
University College London
Roberts Building 1.08 Laboratory, London WC1E 7JE, UK

Prof. J. Ward
The Advanced Center for Biochemical Engineering
Department of Biochemical Engineering
University College London
Room 6.09 Bernard Katz Building, London WC1E 6BT, UK

Prof. K.-L. Choy
Institute for Materials Discovery
Faculty of Maths and Physical Sciences
University College London
Room 1.07 Roberts Building, London WC1E 7JE, UK
E-mail: k.choy@ucl.ac.uk

 The ORCID identification number(s) for the author(s) of this article can be found under <https://doi.org/10.1002/mabi.202000070>.

© 2020 The Authors. Published by WILEY-VCH Verlag GmbH & Co. KGaA, Weinheim. This is an open access article under the terms of the Creative Commons Attribution License, which permits use, distribution and reproduction in any medium, provided the original work is properly cited.

DOI: 10.1002/mabi.202000070

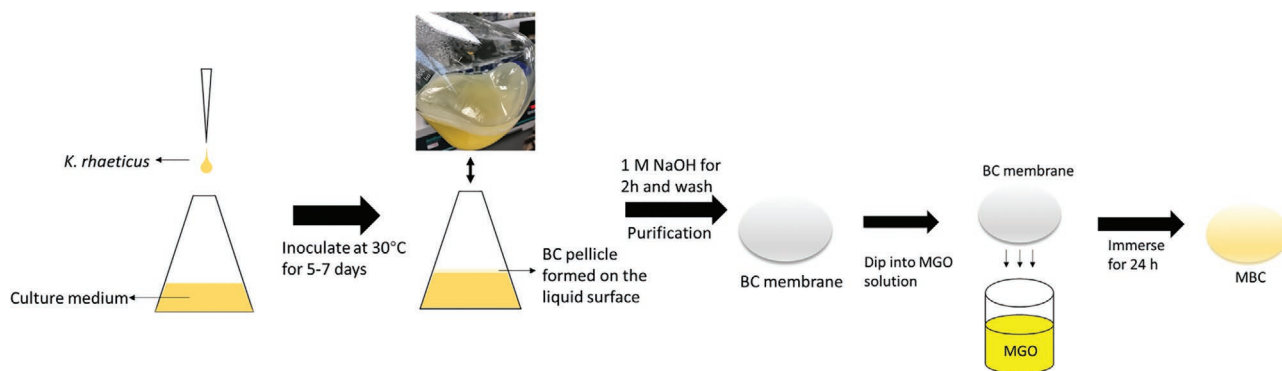


Figure 1. The schematic of BC/MGO fabrication process.

Therefore, there is a need to find a natural material and greener method in antimicrobial BC composite fabrication.

Honey, especially Manuka honey, has been studied as a therapeutic management method of chronic wounds in both in vitro and in vivo research works.^[27–29] Different from plain honey, Manuka honey contains a unique component, methylglyoxal (MGO), which can act as an antimicrobial agent in wound healing process.^[30–33] The antimicrobial property of MGO in the form of a solution,^[34] hydrogel,^[35] polymer and polymer fibers,^[36] nonwoven fabric^[33] have been investigated. It has been found that MGO with the concentration of $0.0054 \text{ mg cm}^{-2}$ was sufficient to reach 100% colony forming

pathogenic bacteria reduction. Rabie et al.^[37] found that MGO can damage the structural integrity and function of bacteria DNA and proteins by disrupting glutathione homeostasis, thus altering the permeability which leads to cellular lysis.

Therefore, inspired by the naturally antimicrobial Manuka honey, it is of great interest to study the degree to which MGO coated BC has antimicrobial property against broad-spectrum bacteria as compared with other antimicrobial BC composites. In this report, we prepared BC/MGO composites by dip-coating MGO solutions onto BC membrane to produce BC/MGO (4%), BC/MGO (0.4%), and BC/MGO (0.04%) samples with different MGO concentrations (v/v in H₂O) (see **Figure 1**

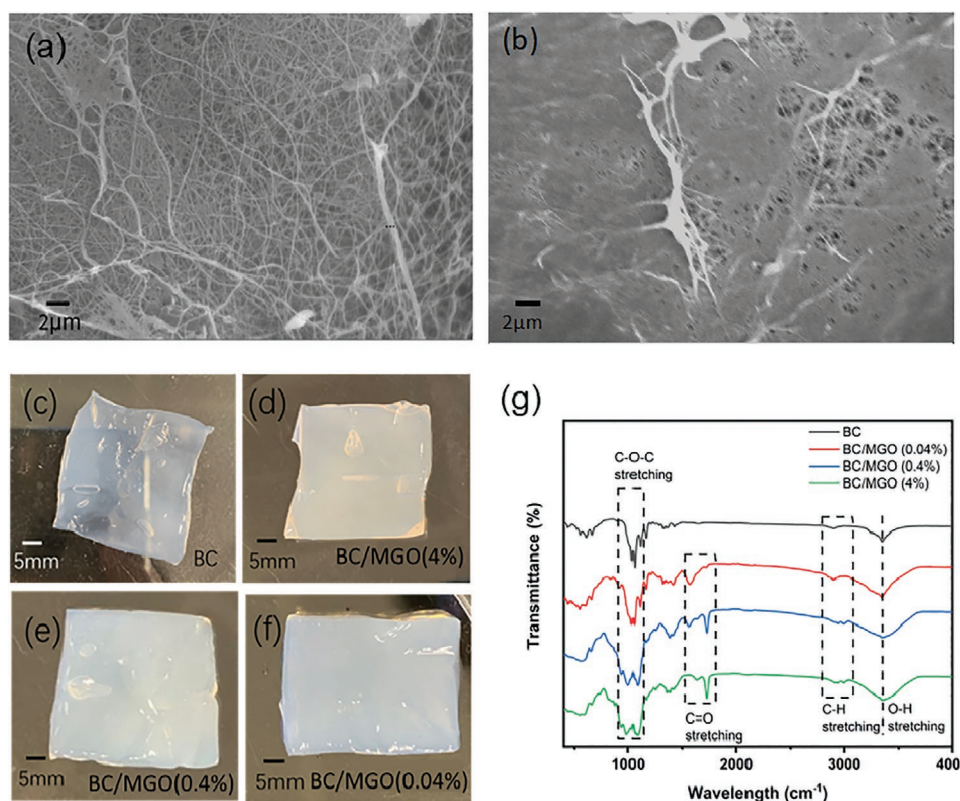


Figure 2. Characterization of nanostructure and elemental composition of BC and BC/MGO. a) SEM image of plain BC after freeze-drying. b) SEM image of MGO coated BC after freeze-drying. And pictures of c) untreated BC and d) BC/MGO samples (BC/MGO (4%), e) BC/MGO (0.4%), f) BC/MGO (0.04%). g) FTIR analysis confirming the presence of MGO in BC.

for the illustration of the fabrication process) and tested against a broad-spectrum of bacteria including Gram-positive *Micrococcus luteus* (*M. luteus*), *Staphylococcus aureus* (*S. aureus*) and Gram-negative *Pseudomonas aeruginosa* (*P. aeruginosa*), *Escherichia coli* (*E. coli*).

2. Results and Discussions

2.1. Structural Characterizations

Photos of pristine BC membrane and BC/MGO composite (Figure 2c–f) indicated that both untreated plain BC and BC/MGO membranes are soft and translucent, while BC/MGO with a higher MGO content showed more yellowish. Scanning electron microscope (SEM) images of MGO/BC confirmed the presence of nanometer fibrils (≈ 60 – 200 nm in diameter) and 3D interconnected structure (Figure 2b), which is in good agreement with the structural characteristics of plain BC (Figure 2a). As compared with plain BC sample, MGO/BC sample indicated that there was a change in the surface morphology where MGO acted as a coating filling the voids and covering the fibril network of the original BC. Fourier transform infrared (FTIR) analysis showed the presence of C–O–C at 980 cm^{-1} , C–H bending at 1088 cm^{-1} ,^[38] C–O stretching, and OH stretching at peaks of 1058.75 and 3351.75 cm^{-1} , indicating the chemical structure of the plain BC.^[39] In addition, the second line in FTIR analysis graph showed the existence of a peak of C=O stretching group at 1750 cm^{-1} ,^[40] which confirmed the incorporation of MGO into the BC.

To further investigate and compare the surface morphology between BC and BC/MGO with different MGO coating concentrations, atomic force microscopy (AFM) characterizations were also conducted. As shown in Figure 3a,b, the mean diameter of the BC fibers was ≈ 50 nm, which is in accordance with other publications.^[41,42] Meanwhile, BC/MGO nanocomposites in Figure 3c–h showed similar fibrils diameter as the plain BC; however, the surface roughness of the nanocomposites increased with increasing MGO content. In this case, Figure 3g,h revealed the most obvious difference in the surface morphology of BC/MGO nanocomposites from the plain BC, where the roughness was the highest, ≈ 114 nm. Furthermore, some knots were observed around the fiber-net, indicating that the incorporation of MGO coating on BC could increase the surface roughness by interpenetrating the nanonetwork structure, caused by the excellent physical absorption property of the interconnected nanonetwork of the plain BC.

2.2. Thermogravimetric Analysis (TGA)

In order to understand the thermal decomposition behavior of BC and BC/MGO composites, TGA was performed. Figure 4 shows the weight loss curves (TG) of BC, BC/MGO (4%), BC/MGO (0.4%), and BC/MGO (0.04%), indicating that there was dehydration below $100\text{ }^{\circ}\text{C}$, depolymerization and decomposition of glucosyl unites from 320 to $400\text{ }^{\circ}\text{C}$.^[43–46] When BC coated with MGO was analyzed using TGA, the nanocomposite was less stable than plain BC, with degradation at 320 – $370\text{ }^{\circ}\text{C}$,

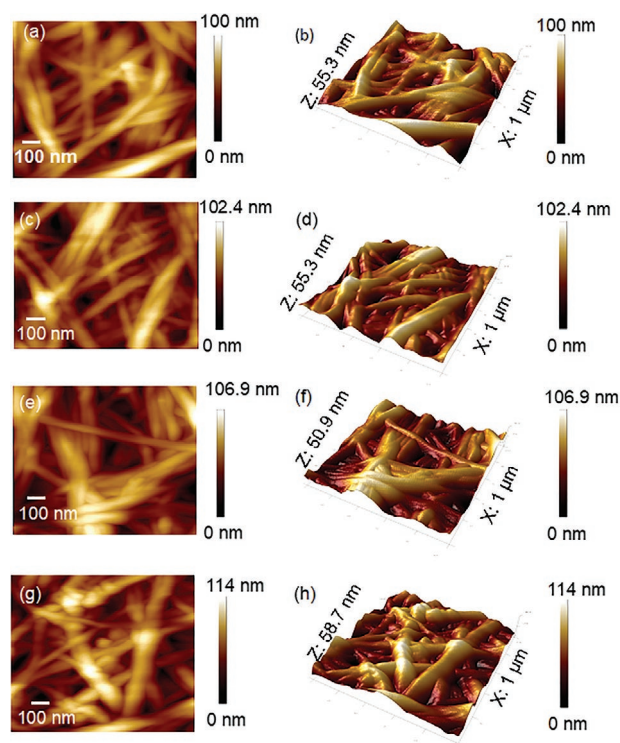


Figure 3. AFM images of a) BC, c) BC/MGO (0.04%), e) BC/MGO (0.4%), and g) BC/MGO (4%) and 3D surface images of b) BC, d) BC/MGO (0.04%), f) BC/MGO (0.4%), and h) BC/MGO (4%).

while plain BC degraded at 380 – $400\text{ }^{\circ}\text{C}$. This may be attributed to the weaker hydrogen bonding and decreased crystallinity when an increasing MGO content was introduced.

2.3. Mechanical Test

As mechanical strength is a key property of materials used in wound dressing applications, the tensile strength was tested in

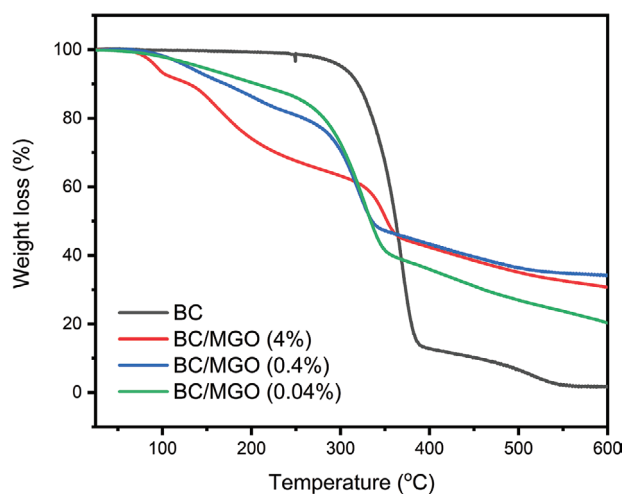


Figure 4. TGA curves of BC, BC/MGO (4%), BC/MGO (0.4%), and BC/MGO (0.04%).

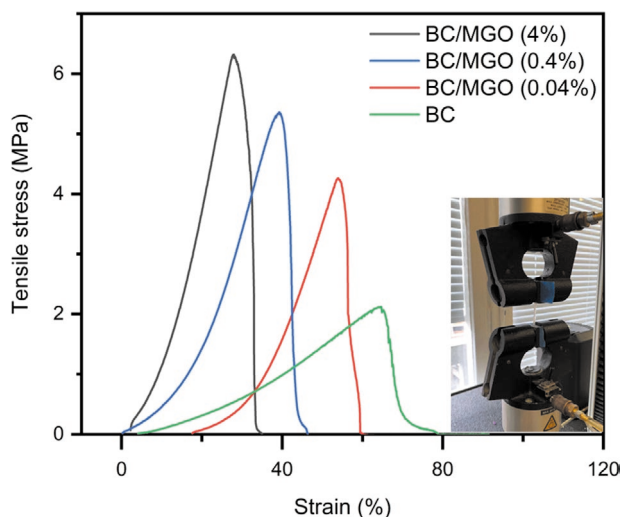


Figure 5. Tensile test to determine the mechanical properties of untreated BC and treated BC (BC/MGO (4%), BC/MGO (0.4%), and BC/MGO (0.04%)).

untreated BC as well as BC/MGO with various MGO concentrations in the wet state. The tensile properties of the samples were illustrated in **Figure 5** and summarized in **Table 1**. BC based samples exhibited high tensile strength due to the interconnected nanonetwork structure with strong hydrogen bonding.^[47] Compared with other BC/MGO samples, untreated BC sample seems to be softer, more ductile, and flexible. Whereas, BC/MGO samples seemed to be harder and more brittle, with the increase of MGO concentration. BC/MGO 4% with the highest coating concentration of MGO exhibited highest tensile strength but lowest extension, which might be attributed to the presence of strongest carbonyl group due to increasing in the crystallinity of materials.^[48] Overall all BC/MGO samples exhibited good mechanical properties, which make them promising flexible wound dressing materials.

2.4. Disk Diffusion Antimicrobial Test

In this work, the antimicrobial property of MGO coated BC nanocomposites against *M. luteus*, *P. aeruginosa*, *S. aureus*, and *E. coli* were investigated by the disk diffusion test method (**Figure 6a–d**). For each plate, a positive control group of two antibiotics dipped BC and plain BC control group were tested as comparison. The efficiency of antimicrobial activity was measured by the diameter of clear zones of inhibition (DIZ) around the round-shaped cut samples after 24 h of incubation

Table 1. Mechanical properties of untreated BC, BC/MGO (4%), BC/MGO (0.4%) and BC/MGO (0.04%) samples.

Materials	Thickness [mm]	Tensile strength [MPa]	Elongation [%]
Untreated BC	0.638 ± 0.035	2.02 ± 0.229	63.8 ± 1.453
BC/MGO (4%)	0.547 ± 0.017	6.32 ± 0.231	29.59 ± 0.768
BC/MGO (0.4%)	0.508 ± 0.019	5.13 ± 1.640	38.97 ± 1.859
BC/MGO (0.04%)	0.671 ± 0.015	4.36 ± 1.341	55.33 ± 1.596

in 37 °C. After 24 h incubation, DIZ of BC/MGO (4%) with highest MGO concentration were investigated as 14.3 ± 1.3, 12.3 ± 0.3, 17.1 ± 0.6, and 15.5 ± 0.5 mm in **Figure 6e**, while the positive control groups were 12.7 ± 1.4, 10.0 ± 0.5, 5.2 ± 0.4, and 8.5 ± 1 mm, and control groups of plain BC were none for all the samples, against *M. luteus*, *P. aeruginosa*, *S. aureus*, and *E. coli*, respectively. In addition, it was also obvious from **Figure 6e** that BC/MGO nanocomposites were slightly more effective on Gram-positive than biofilm contained Gram-negative bacteria strains while it was still lethal to multiantibiotic-resistant *S. aureus*. The results showed that for all these bacteria strains, with the increase of MGO concentrations, the antimicrobial activity was more pronounced. This indicated that MGO coated BC, with at least 0.04% concentration, sufficient to reduce the activity of most pathogenic bacteria which are the most likely

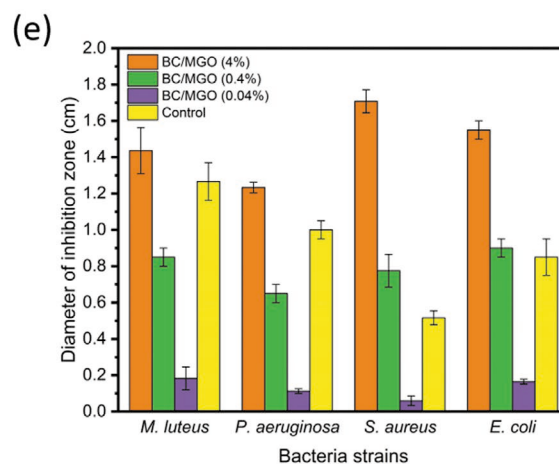
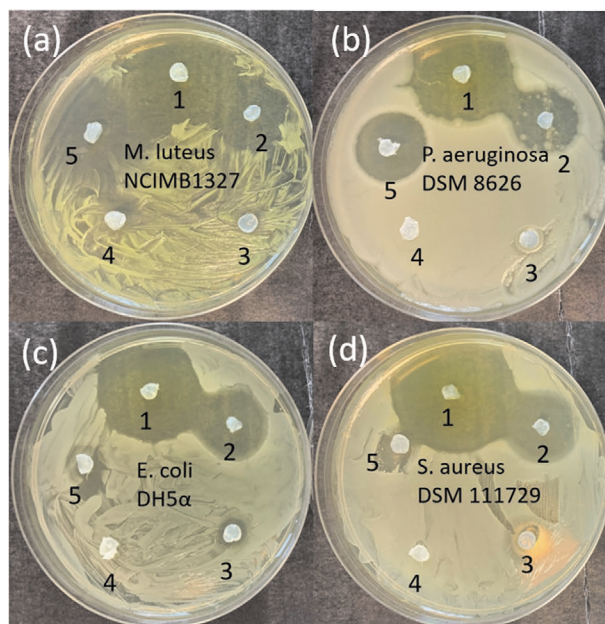


Figure 6. Disk diffusion test of MGO/BC samples against a) *M. luteus*, b) *P. aeruginosa*, c) *S. aureus*, and d) *E. coli* (sample number 1: BC/MGO (4%), 2: BC/MGO(0.4%), 3: BC/MGO(0.04%), 4: plain BC, and 5: antibiotics positive control (kanamycin (50 mg mL⁻¹) for (a) and (b) and ampicillin (50 mg mL⁻¹) for (c) and (d)). e) Diameter of inhibition zone measured of each sample against different bacteria strains.

Table 2. Summary of common wound dressing materials in recent literatures.

	Materials	Diameter of zone of inhibition (DIZ) [mm]		Type of wounds applications
		<i>E. coli</i>	<i>S. aureus</i>	
Nanoparticle based nanocomposites	Chitosan/gelatin/Fe ₃ O ₄ nanofiber membrane ^[49]	21 ± 1	20 ± 2	Normal wounds
	Chitosan/poly(<i>N</i> -vinylpyrrolidone)/TiO ₂ nanocomposite ^[50]	30 ± 0	32 ± 0	Infected wounds
	Alginate hydrogel/zinc oxide nanoparticles composite ^[51]	16 ± 1	18 ± 2	Infected wounds
	Chitosan–hyaluronic acid/nanosilver composite sponge ^[52]	13 ± 2	14 ± 2 10 ± 2 for MRSA	Diabetic wounds
	Silver nanoparticles hydrogel ^[53]	10.4 ± 0.7	10.8 ± 0.7	Burn wounds
Natural antibacterial agents based composites	<i>Lawsonia Inermis</i> -gelatin-starch nanofibrous dressing ^[54]	4.45 ± 0.13	3.34	Burn wounds
	Hypericum perforatum/chitosan films ^[55]	2.9 ± 0.1	1.97 ± 0.05	Normal wounds
	Curcumin nanocomposite ^[56]	19 ± 0	14 ± 0	Infected wounds
	Poly(ϵ -caprolactone)/poly(lactic acid)/thymol nanofibrous mats ^[57]	7.8 ± 0	10.4 ± 0	Normal wounds
BC based nanocomposites	BC/tetracycline hydrochloride (TCH) ^[25]	47.5 ± 0	38.5 ± 0	Infected wounds
	BC/antibiotic fusidic acid (FA) ^[58]	–	30 ± 0	Infected wounds
	BC/copper nanoparticle ^[59]	21.3 ± 1.5	20.0 ± 0.8	Long-term infected wounds
	BC/zinc oxide ^[60]	27 ± 0	28.6 ± 1.15	Burn wounds
	BC/silver nanoparticle ^[61]	2.03 ± 0	3.46 ± 0	Normal wounds
Silver-based commercial wound dressings	Silver sulfadiazine ^[62]	9.3 ± 0	13 ± 0	Infected wounds
	Acticoat ^[62]	9.7 ± 0	10.3 ± 0	
The proposed BC/MGO nanocomposite	BC/MGO nanocomposite	15.5 ± 0.5	17.1 ± 0.6	Chronic wounds

to exist in the mid to late stage of chronic wounds. **Table 2** summarized recent publications on antimicrobial property of wound dressing materials including BC based nanocomposite. The different values of DIZ against *E. coli* and *S. aureus* can be used to make comparisons. Although it cannot be comparable with antiseptic or antibiotic based BC composites, BC/MGO is still among the best in BC related antimicrobial materials. In addition, it is also of great significance to compare BC/MGO nanocomposite with other antimicrobial wound dressing materials. It is indicated that our proposed BC/MGO composite is among the best in natural antibacterial agents based and commercial silver based wound dressing materials against *E. coli* and *S. aureus*, though it is less effective than some nanoparticle embedded composites. Therefore, it can be confirmed that MGO/BC has great potential application in bacteria-infectious chronic wound dressing applications.

3. Conclusion

In this paper, we proposed an ecofriendly, nature-inspired, and cost-effective nanocomposite for chronic wounds dressing, made by antimicrobial BC/MGO nanocomposite via a simple dip-coating method. SEM and AFM characterizations indicated the difference in surface morphology of the interconnected

nanostructure between BC and MGO, and FTIR analysis confirmed the introduction of MGO onto BC. Thermal analysis test revealed the great thermal stability of both BC and BC/MGO; however, there was a slight reduction in the thermal stability of BC/MGO composite possibly due to the reduction of hydrogen bonds and increase of crystallinity. Despite this slight reduction in thermal stability, this should not affect the practical application of BC/MGO composite as a promising wound dressing material which is normally used at human body temperature (37 °C). Disk diffusion test showed BC/MGO based composites exhibited high antibacterial effect against most common pathogens in chronic wounds, even against antibiotic-resistant *S. aureus*, compared with other antimicrobial wound dressing composites in other publications. Tensile tests confirmed the excellent mechanical strength of BC/MGO composite. All these render BC/MGO composite a potential material for chronic wound dressings or skin substitute in chronic wound bed.

4. Experimental Section

Materials: All chemicals were obtained from Sigma-Aldrich (USA). *Komagataeibacter rhaeticus* DSM16663, *Micrococcus luteus* NCIMB8628, *Pseudomonas aeruginosa* NCIMB1327, *Staphylococcus aureus* DSM111729, and *Escherichia coli* DH5 α bacteria strains were kindly provided by



Professor John Ward. The BC membranes were punched into discs of 6 mm diameter using a biopsy punch (Stiefel, UK) and stored in 90% ethanol prior to use. Cell culture medium was supplied from Sigma-Aldrich (USA).

BC Inoculation and BC/MGO Sample Fabrication: *Komagataeibacter rhaeticus* DSM 16663 was cultured in the *Gluconacetobacter rhaeticus* medium (5% glucose, 5% yeast extract, and 1 L deionized (DI) water with pH adjusted to 6.5) in a 30 °C incubator for 3–5 d. Then BC pellicles were taken out and heated in 1 M NaOH solution at 75 °C for 2 h. After washing with DI water until the pH was neutral, the BC membrane preparation was complete and cut into 3 cm × 3 cm square. BC membranes were dip coated into 20 mL 4% v/v MGO solution to make sample BC/MGO (4%), followed by diluting the MGO concentration into 0.4% v/v and 0.04% v/v, resulting in BC/MGO (4%), BC/MGO (0.4%), and BC/MGO (0.04%). After storing in fridge for 24 h the samples were cut into 3 cm × 3 cm square-shape pieces.

Characterizations: A ZEISS Ultra 55 field emission gun SEM was used to characterize the surface morphology of BC and BC/MGO based nanocomposites. Prior to investigation, each sample was subjected to a freeze-drying process in liquid nitrogen (−195 °C) and subsequently gold coated with a thickness of average 15 nm using a gold sputter. Surface morphology of samples was also characterized by AFM in a tapping mode. The composition of BC and BC/MGO composite was characterized by FTIR spectroscopy (Perkin Elmer, USA) at wavelength from 400 to 4000 cm^{−1}. TGA test was carried out using a Perkin-Elmer 2000 instrument, under continuous nitrogen flow of 70 mL min^{−1}, and a 10 mg sample was used and the weight loss was recorded from 25 to 600 °C with temperature ramp at 10 °C min^{−1}. Mechanical test was performed by Instron tensile tester, according to active standard test method D638 equipped with 1 kN static load cell. During the test, the tensile strength and elongation at break can be calculated based on measured thickness and width of each sample. A test speed of 10 mm min^{−1} was used. Each sample was tested at least five times.

Antimicrobial Activity: The antimicrobial activity of BC/MGO composites was investigated by disk diffusion test against *M. luteus* (NCIMB1327), *P. aeruginosa* (DSM8626), *S. aureus* (DSM111729), and *E. coli* (DH5α). Prior to the test, BC and BC/MGO samples were punched into 6 mm round-shaped discs. The tests were performed according to the standard Kirby–Bauer Disk Diffusion Susceptibility Test Protocol (American Society of Microbiology, 2009). Lawns of test bacteria (about 1 × 10⁵ CFU per plate) were prepared from Luria-Bertani Broth cultivation overnight. The composites, positive control samples dipped with Kanamycin (50 mg mL^{−1}) and Ampicillin (50 mg mL^{−1}) and plain BC control groups were put onto the bacteria-spread agar plates and marked. After 24 h incubation at 37 °C, the plates were taken out and the diameter of inhibitions zones was measured with a ruler. The tests were done in triplicate.

Acknowledgements

The authors would like to thank Jinke Chang and Fan Cui for their help in performing Instron tensile test and AFM characterization. All authors contributed to the experimental design and data analyses. The paper was written through contributions of all authors. All authors have given approval to the final version of the paper.

Conflict of Interest

The authors declare no conflict of interest.

Keywords

antimicrobial, biomaterial, nanomaterial, nature-inspired, wound healing

Received: March 9, 2020

Revised: May 7, 2020

Published online:

- [1] F. Esa, S. M. Tasirin, N. A. Rahman, *Ital. Oral Surg.* **2014**, *2*, 113.
- [2] P. Chen, S. Y. Cho, H.-J. Jin, *Macromol. Res.* **2010**, *18*, 309.
- [3] O. Saibuatong, M. Phisalaphong, *Carbohydr. Polym.* **2010**, *79*, 455.
- [4] Y. Dahman, K. E. Jayasuriya, M. Kalis, *Appl. Biochem. Biotechnol.* **2010**, *162*, 1647.
- [5] C. Castro, R. Zuluaga, J. L. Putaux, G. Caro, I. Mondragon, P. Gañán, *Carbohydr. Polym.* **2011**, *84*, 96.
- [6] S. M. Keshk, *J. Bioprocess. Biotech.* **2014**, *04*, 1.
- [7] S. J. Eichhorn, C. A. Baillie, N. Zafeiropoulos, L. Y. Mwaikambo, M. P. Ansell, A. Dufresne, K. M. Entwistle, P. J. Herrera-Franco, G. C. Escamilla, L. Groom, M. Hughes, C. Hill, T. G. Rials, P. M. Wild, *J. Mater. Sci.* **2001**, *36*, 2107.
- [8] D. Klemm, D. Schumann, U. Udhardt, S. Marsch, *Prog. Polym. Sci.* **2001**, *26*, 1561.
- [9] C. R. Rambo, D. O. S. Recouvreur, C. A. Carminatti, A. K. Pitlovanciv, R. V. Antônio, L. M. Porto, *Mater. Sci. Eng., C* **2008**, *28*, 549.
- [10] N. Shah, M. Ul-Islam, W. A. Khattak, J. K. Park, *Carbohydr. Polym.* **2013**, *98*, 1585.
- [11] T. Maneerung, S. Tokura, R. Rujiravanit, *Carbohydr. Polym.* **2008**, *72*, 43.
- [12] Q. Lin, Y. Zheng, L. Ren, J. Wu, H. Wang, J. An, W. Fan, *J. Appl. Polym. Sci.* **2014**, *131*, 1.
- [13] W. Czaja, A. Krystynowicz, S. Bielecki, R. M. Brown, Jr., *Biomaterials* **2006**, *27*, 145.
- [14] M. Ramos-e-silva, M. Cristina, R. D. E. Castro, *Clin. Dermatol.* **2002**, *20*, 715.
- [15] D. Simões, S. P. Miguel, M. P. Ribeiro, P. Coutinho, A. G. Mendonça, I. J. Correia, *Eur. J. Pharm. Biopharm.* **2018**, *127*, 130.
- [16] E. M. Ahmed, *J. Adv. Res.* **2015**, *6*, 105.
- [17] E. A. Kamoun, E. R. S. Kenawy, X. Chen, *J. Adv. Res.* **2017**, *8*, 217.
- [18] F. S. Pott, M. J. Meier, J. G. D. Stocco, K. Crozeta, J. D. Ribas, *Rev. Lat.-Am. Enferm.* **2014**, *22*, 511.
- [19] P. Zahedi, I. Rezaei, S. O. Ranaei-Siadat, S. H. Jafari, P. Supaphol, *Polym. Adv. Technol.* **2010**, *21*, 77.
- [20] W. Hu, S. Chen, X. Li, S. Shi, W. Shen, X. Zhang, H. Wang, *Mater. Sci. Eng., C* **2009**, *29*, 1216.
- [21] K.-H. Cho, J.-E. Park, T. Osaka, S.-G. Park, *Electrochim. Acta* **2005**, *51*, 956.
- [22] M. K. Temgire, S. S. Joshi, *Radiat. Phys. Chem.* **2004**, *71*, 1039.
- [23] R. J. B. Pinto, S. Daina, P. Sadocco, C. P. Neto, T. Trindade, *Biomed Res. Int.* **2013**, *2013*, 1.
- [24] C. Wiegand, S. Moritz, N. Hessler, D. Kralisch, D. Fischer, U. Hipler, *J. Mater. Sci.: Mater. Med.* **2015**, *26*, 1.
- [25] W. Shao, H. Liu, S. Wang, J. Wu, M. Huang, H. Min, X. Liu, *Carbohydr. Polym.* **2016**, *145*, 114.
- [26] R. B. James, D. William, T. G. Berger, D. M. Elston, Odorn, *Andrews Dis. Skin: Clin. Dermatol.* **2011**.
- [27] G. Gethin, S. Cowman, *Case Study* **2005**, *2*, 10.
- [28] D. W. Johnson, C. Van Eps, D. W. Mudge, K. J. Wiggins, K. Armstrong, C. M. Hawley, S. B. Campbell, N. M. Isbel, G. R. Nimmo, H. Gibbs, *J. Am. Soc. Nephrol.* **2005**, *16*, 1456.
- [29] L. Rafter, T. Reynolds, M. Collier, M. Rafter, M. West, *Wounds UK* **2017**, *13*, 132.
- [30] R. Jenkins, N. Burton, R. Cooper, *Int. J. Antimicrob. Agents* **2011**, *37*, 373.
- [31] A. G. Leong, P. M. Herst, J. L. Harper, *Innate Immun.* **2012**, *18*, 459.
- [32] C. J. Adams, M. Manley-Harris, P. C. Molan, *Carbohydr. Res.* **2009**, *344*, 1050.

- [33] S. E. L. Bulman, G. Tronci, P. Goswami, C. Carr, S. J. Russell, *Materials* **2017**, *10*, 954.
- [34] E. Mavric, S. Wittmann, G. Barth, T. Henle, *Mol. Nutr. Food Res.* **2008**, *52*, 483.
- [35] M. Fidaleo, A. Zuorro, R. Lavecchia, *Chem. Lett.* **2010**, *39*, 322.
- [36] S. Ghosh, P. Chakraborty, P. Saha, S. Acharya, M. Ray, *RSC Adv.* **2014**, *4*, 23251.
- [37] E. Rabie, J. C. Serem, H. M. Oberholzer, A. R. M. Gaspar, M. J. Bester, *Ultrastruct. Pathol.* **2016**, *40*, 107.
- [38] R. Auta, *Afr. J. Biotechnol.* **2017**, *16*, 470.
- [39] Y. J. Choi, Y. Ahn, M. S. Kang, H. K. Jun, I. S. Kim, S. H. Moon, *J. Chem. Technol. Biotechnol.* **2004**, *79*, 79.
- [40] S. Islam, A. R. Mir Moinuddin, M. Y. Arfat, K. Alam, A. Ali, *Int. J. Biol. Macromol.* **2017**, *104*, 19.
- [41] K. Y. Lee, A. Bismarck, *Cellulose* **2012**, *19*, 891.
- [42] A. Mautner, K. Y. Lee, T. Tammelin, A. P. Mathew, A. J. Nedoma, K. Li, A. Bismarck, *React. Funct. Polym.* **2015**, *86*, 209.
- [43] M. Roman, W. T. Winter, *Biomacromolecules* **2004**, *5*, 1671.
- [44] J. George, K. V. Ramana, A. S. Bawa, Siddaramaiah, *Int. J. Biol. Macromol.* **2011**, *48*, 50.
- [45] S. Gea, C. T. Reynolds, N. Roohpour, B. Wirjosentono, N. Soykeabkaew, E. Bilotti, T. Peijs, *Bioresour. Technol.* **2011**, *102*, 9105.
- [46] Y. Jia, X. Wang, M. Huo, X. Zhai, F. Li, C. Zhong, *Nanomater. Nanotechnol.* **2017**, *7*, 1.
- [47] Z. Yan, S. Chen, H. Wang, B. Wang, J. Jiang, *Carbohydr. Polym.* **2008**, *74*, 659.
- [48] J. Xiong, K. Ni, X. Liao, J. Zhu, Z. An, Q. Yang, Y. Huang, G. Li, *Polym. Int.* **2016**, *65*, 1474.
- [49] N. Cai, C. Li, C. Han, X. Luo, L. Shen, Y. Xue, F. Yu, *Appl. Surf. Sci.* **2016**, *369*, 492.
- [50] D. Archana, B. K. Singh, J. Dutta, P. K. Dutta, *Carbohydr. Polym.* **2013**, *95*, 530.
- [51] A. Mohandas, *Int. J. Nanomed.* **2019**, *14*, 2607.
- [52] B. S. Anisha, R. Biswas, K. P. Chennazhi, R. Jayakumar, *Int. J. Biol. Macromol.* **2013**, *62*, 310.
- [53] B. Boonkaew, P. M. Barber, S. Rengpipat, P. Supaphol, M. Kempf, J. He, V. T. John, L. Cuttle, *J. Pharm. Sci.* **2014**, *103*, 3244.
- [54] Z. Hadisi, J. Nourmohammadi, S. M. Nassiri, *Int. J. Biol. Macromol.* **2018**, *107*, 2008.
- [55] S. Güneş, F. Tihminlioğlu, *Int. J. Biol. Macromol.* **2017**, *102*, 933.
- [56] G. D. Venkatasubbu, T. Anusuya, *Int. J. Biol. Macromol.* **2017**, *98*, 366.
- [57] Z. Karami, I. Rezaeian, P. Zahedi, M. Abdollahi, *J. Appl. Polym. Sci.* **2013**, *129*, 756.
- [58] K. Aschberger, S. Gottardo, *J. Phys.: Conf. Ser.* **2017**, *755*, 011001.
- [59] W. He, X. Huang, Y. Zheng, Y. Sun, Y. Xie, Y. Wang, L. Yue, *J. Biomater. Sci., Polym. Ed.* **2018**, *29*, 2137.
- [60] A. Khalid, R. Khan, M. Ul-Islam, T. Khan, F. Wahid, *Carbohydr. Polym.* **2017**, *164*, 214.
- [61] J. Wu, Y. Zheng, X. Wen, Q. Lin, X. Chen, Z. Wu, *Biomed. Mater.* **2014**, *9*, 035005.
- [62] C. L. Gallant-Behm, H. Q. Yin, S. Liu, J. P. Hegggers, E. Langford, M. E. Olson, D. A. Hart, R. E. Burrell, *Wound Repair Regen.* **2005**, *13*, 412.